Geophysical Journal International

Geophys. J. Int. (2017) **211,** 1414–1427
Advance Access publication 2017 September 7
GJI Seismology

doi: 10.1093/gji/ggx373

Heat flow, seismic cut-off depth and thermal modeling of the Fennoscandian Shield

Toni Veikkolainen,[1] Ilmo T. Kukkonen[1] and Timo Tiira[2]

[1]*Department of Physics, University of Helsinki, P.O. Box 68, FI-00014 Helsinki, Finland. E-mail: toni.veikkolainen@helsinki.fi*
[2]*Institute of Seismology, University of Helsinki, P.O. Box 68, FI-00014 Helsinki, Finland*

Accepted 2017 September 6. Received 2017 July 11; in original form 2017 April 11

SUMMARY

Being far from plate boundaries but covered with seismograph networks, the Fennoscandian Shield features an ideal test laboratory for studies of intraplate seismicity. For this purpose, this study applies 4190 earthquake events from years 2000–2015 with magnitudes ranging from 0.10 to 5.22 in Finnish and Swedish national catalogues. In addition, 223 heat flow determinations from both countries and their immediate vicinity were used to analyse the potential correlation of earthquake focal depths and the spatially interpolated heat flow field. Separate subset analyses were performed for five areas of notable seismic activity: the southern Gulf of Bothnia coast of Sweden (area 1), the northern Gulf of Bothnia coast of Sweden (area 2), the Swedish Norrbotten and western Finnish Lapland (area 3), the Kuusamo region of Finland (area 4) and the southernmost Sweden (area 5). In total, our subsets incorporated 3619 earthquake events. No obvious relation of heat flow and focal depth exists, implying that variations of heat flow are primarily caused by shallow lying heat producing units instead of deeper sources. This allows for construction of generic geotherms for the range of representative palaeoclimatically corrected (steady-state) surface heat flow values (40–60 mW m^{-2}). The 1-D geotherms constructed for a three-layer crust and lithospheric upper mantle are based on mantle heat flow constrained with the aid of mantle xenolith thermobarometry (9–15 mW m^{-2}), upper crustal heat production values (3.3–1.1 μWm^{-3}) and the brittle-ductile transition temperature (350 °C) assigned to the cut-off depth of seismicity (28 ± 4 km). For the middle and lower crust heat production values of 0.6 and 0.2 μWm^{-3} were assigned, respectively. The models suggest a Moho temperature range of 460–500 °C.

Key words: Heat flow; Europe; Spatial analysis; Statistical seismology; Cratons; Crustal structure.

1 INTRODUCTION

The maximum focal depth (i.e. cut-off depth) of earthquakes has been frequently used to model thermal conditions of the lithosphere, especially to approximate the depth below which the ductile transformation dominates over brittle transformation of the crust. This depth, useful for the verification of rheological models, has been usually considered a temperature isotherm. However, widely varying temperature estimates have been given for it, ranging from 260 ± 40 up to 450 ± 50 °C depending on the tectonothermal setting and the crustal lithologies of the area (Ranalli 1995; Bonner *et al.* 2003). However, the temperature of 350 °C has been considered a viable choice for Fennoscandia, given the dominance of felsic rocks in its upper and middle crust (Blanpied *et al.* 1991; Moisio 2005) and the tendency of even small concentrations of liquid water to decrease the lithospheric strength (Mackwell *et al.* 1998) at temperatures close to the critical point of water (374 °C at 22 MPa). The lithological composition of the crust is, however, not simple. Kuusisto *et al.* (2006) modeled the crustal seismic velocity structures in the central part of the Fennoscandian shield using mixtures of different lithologies for the different velocity layers and concluded that quartz-bearing rock types are abundant from the surface down to the depth of 25–30 km. The calculated models suggested that the crustal velocity profiles can be simulated with rock-type mixtures where the upper crust consists of felsic gneisses and granitic–granodioritic rocks with a minor contribution of amphibolite and diabase. In the middle crust, the amphibolite proportion increases. The lower crust consists of tonalitic gneiss, mafic garnet granulite, hornblendite, pyroxenite and minor mafic eclogite. If the lithospheres were mafic or ultramafic, the brittle-ductile transition would occur at a greater temperature than the range of 300–400 °C assigned for granitic (quartz-bearing) lithology (Blanpied *et al.* 1991).

Correlation between the basal depth of the seismogenic zone and the terrestrial heat flow has been studied both in intraplate areas (Bollinger *et al.* 1985; Klemperer 1987; Wong & Chapman 1990)

and in the proximity of plate margins (Tanaka & Ishikawa 2002; Bonner *et al.* 2003). For example, the Japanese data (Tanaka 2004; Tanaka *et al.* 2004) obviously show a shift from volcanic areas with high heat flow and focal depths less than 5 km to mountain ranges with low heat flow and focal depths more than 30 km. In several shield areas, the rarity of earthquake events, the concentration of heat producing elements at shallow depths, and also the spatially insufficient distribution of geothermal gradient and thermal conductivity measurements may impair attempts to correlate earthquake depths with heat flow. In the Fennoscandian Shield, the distribution of seismic events is uneven and is densest at intraplate ('postglacial') faults (Lagerbäck & Sundh 2008) which are a result of rapid removal of ice load at the end-stage of the Weichselian glaciation about 9000 yr ago. A combination of postglacial isostatic adjustment, ridge push from distant plate boundaries and the rapid change in the stress field was responsible of the faulting (Lund 2005; Lund *et al.* 2009; Kukkonen *et al.* 2010; Korja *et al.* 2016). The heat flow field of the area is also relatively well constrained, with palaeoclimatically corrected values ranging from 35.3 ± 6.3 mW m^{-2} in Archean areas to 81.6 ± 13.9 mW m^{-2} in post-Sveconorwegian granites (Slagstad *et al.* 2009). The assessment of seismic hazard in potential nuclear power plant construction and waste management sites is one of the most important applications of seismicity studies in areas like this (Bödvarsson *et al.* 2006; Tiira *et al.* 2016).

Our study area is geologically dominated by Archaean crust in the Karelia and Kola cratons in the east and Proterozoic Svecofennian/Sveconorwegian accretionary crust in the west. In northern Finland, the Lapland granulite belt delineates the Karelia-Kola boundary (Lehtinen *et al.* 2006). South of Finland, the Precambrian basement dips below younger sedimentary rocks, with the thickness of the cover being 100–200 m in northern and over 800 m in southeastern Estonia (Puura & Vaher 1997). The Swedish islands of Gotland and Öland are also covered by sediments on crystalline basement. In the far southern Sweden, the Trans-European Suture Zone marks the boundary between the Precambrian eastern Europe and the Phanerozoic western Europe, and in the west, the Caledonian orogeny is predominant (Torsvik & Rehnström 2003; Lahtinen 2012). Although the vast majority of our earthquake data has been obtained from areas with Precambrian lithology, our heat flow mapping covers the entire Finland, Sweden and adjacent areas of Norway, Estonia and Russia, extending from 54.5° to 71.0°N, and from 7.0° to 36.0°E.

2 HEAT FLOW

Gathering heat flow data from Finland and Sweden for mapping was the first essential part of our analysis. Russian, Norwegian, Danish and Estonian data from the vicinity were also included in our compilation because our aim was to interpolate a heat flow surface which should be adequately constrained also in the Finnish and Swedish border regions. Typically heat flow determinations originate from research papers (e.g. Landström *et al.* 1980; Kukkonen 1989a; Jõeleht & Kukkonen 1996; Kukkonen *et al.* 2011) and catalogues (e.g. Eriksson & Malmqvist 1979; Eliasson *et al.* 1991; Davies & Davies 2010) but also from a thesis work (Kukkonen 1989b). Soviet catalogued data from Karelia and Kola were gathered from the East European craton data compilation of Kukkonen & Jõeleht (2003). In Finland and Russia, borehole measurements have been by far the most important way to determine heat flow, but in parts of Norway and Sweden, measurements of lake sediments have been also carried out. We excluded the lake sediment values which were rejected by Slagstad *et al.* (2009) as being unreliable when compared to nearby borehole measurements.

To investigate heat flow throughout our study region, we applied radial basis function interpolation in Scientific Python to construct a heat flow map. Unlike spherical splines, our method does not optimize the smoothness of the surface with the expense of data integrity. On the contrary, the value of the function at data point coordinates is exactly that of the data point itself, and values of the interpolation surface do not fall outside the actual data range. The size of our interpolation grid was 0.05° in both latitude and longitude dimensions, yet an area of a grid cell (in km^2) is not preserved, since latitude circles are shorter at high latitudes. In our analysis, this was no problem as long as the grid size was fine enough to allow a reasonable correlation with earthquake focal coordinates. For the few borehole data with same coordinates (e.g. Fjällväden 1 and 2 in Sweden; Hurter & Hänel 2002), we calculated the arithmetic mean of uncorrected heat flow values before interpolation because our interpolation algorithm did not allow different data values at similar locations. After gathering all heat flow data (223 points; Appendix A), we applied our interpolation to construct a map from palaeoclimatically corrected heat flow determinations (Fig. 1).

In Fennoscandia, palaeoclimate is the most important factor to cause deviations from true steady-state heat flow conditions, but locally adjusted palaeoclimatic corrections can be remarkably different from regional ones. For example, Majorowicz & Wybraniec (2010) suggested a correction of 16–18 mW m^{-2} for surface heat flow data of eastern Finland, but corrections listed by Slagstad *et al.* (2009) are lower, typically less than 10 mW m^{-2}. For the majority of Finnish data, Slagstad *et al.* (2009) apparently applied corrections calculated by Kukkonen (1989b), yet these had notable variations related to local conditions and depths of holes. For example, correction assigned for the Kotalahti borehole is 11 mW m^{-2} and that of Pielavesi hole is −4 mW m^{-2} although these holes are only 85 km apart. On the other hand, Kukkonen (1989b) calculated the mean heat flow of Finland to be 37.0 ± 1.6 mW m^{-2} (uncorrected) and 40.7 ± 1.8 mW m^{-2} (corrected), these values being very close to each other. They had no information from holes deeper than about 1100 m, although deep holes are the only ones which can truthfully record the entire depth range of thermal gradient perturbation from glaciation–deglaciation cycle. Subsequently, Kukkonen*et al.* (1998) reported exceptionally low heat flow values of 2.4–11.6 mW m^{-2} at the depth of 250–750 m in Archean rocks in Russian Karelia. The data were attributed to very cold conditions (permafrost) during the Weichselian glaciation and early deglaciation of the area. To make these heat flow values comparable to other Archaean areas, the palaeoclimatic corrections should have exceeded 20–30 mW m^{-2} (Rudnick & Nyblade 1999; Mareschal & Jaupart 2013).

Whenever possible, palaeoclimatic corrections should be determined for each point separately, since they are strongly dependent on the measurement depth interval of thermal gradient, and the climatic effect also needs to be distinguished from other phenomena which can strongly affect the temperature of the borehole or the well (Mottaghy *et al.* 2005). Therefore interpolating a heat flow correction map from readily corrected borehole data to estimate corrections for other holes (Slagstad *et al.* 2009) in a certain area may result in misleading corrections if measurement depths of uncorrected holes are not taken into account. The typical range of corrections in the interpolated map of Slagstad *et al.* (2009) is, despite this caveat, closer to corrections derived for individual holes (e.g. Kukkonen 1989b) than to the range of regionally determined corrections in the pan-European heat flow study (Majorowicz & Wybraniec 2010).

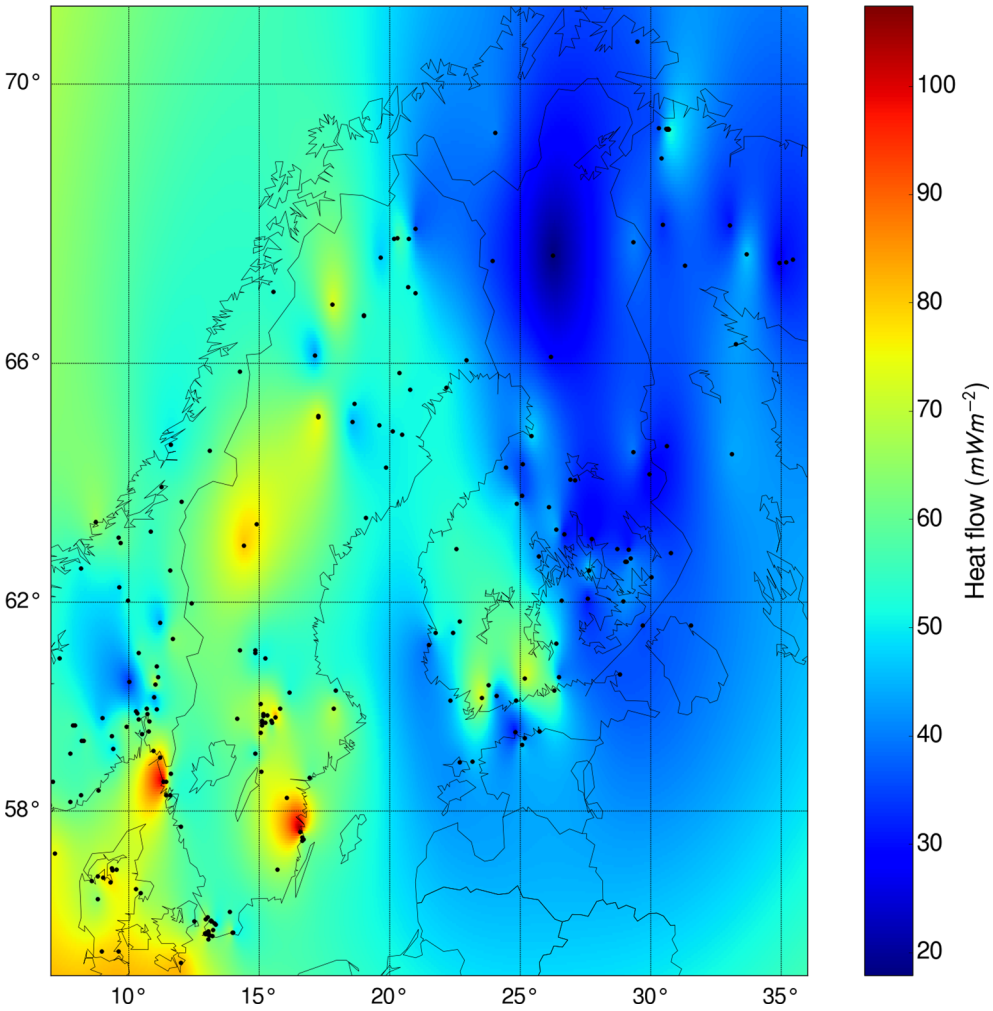

Figure 1. Palaeoclimatically corrected heat flow map of Finland, Sweden and adjacent areas. Data from Appendix A.

The determination of corrections to all holes individually requires detailed information about the climatic history of Fennoscandia and is beyond the scope of this paper. Therefore, we opted for using the correction method of Slagstad *et al.* (2009) on the heat flow versus depth relationship. Unfortunately, the correction map does not cover the eastern and northern parts of Fennoscandia, yet the 2516 m deep Outokumpu deep hole (Kukkonen *et al.* 2011) shows the increase of heat flow from 28 to 32 mW m^{-2} at shallow depths to 40–45 mW m^{-2} near the bottom of the hole. Therefore, correction of *ca.* 10 mW m^{-2} is suggested by Kukkonen *et al.* (2011) for holes not deeper than 1000 m in eastern Fennoscandia. Unlike in the case of Kola superdeep hole (Kukkonen & Clauser 1994; Mottaghy *et al.* 2005), it is likely that advection and structural effects play minimal role in the heat flow of Outokumpu. Although it is not always easy to quantify the relative effects of different aspects which influence the temperature signal, the general increase of heat flow with depth is a phenomenon observed throughout the East European Craton (Kukkonen & Jõeleht 2003). Using Outokumpu result as a proxy, we applied the bulk correction of 10 mW m^{-2} also for 25 other Archean and two Proterozoic data entries which did not have other correction parameters associated with them. Because 26 of these heat flow determinations are located on the Russian territory where none of our earthquake epicentres are located, this kind of adjustment does not seriously alter heat flow field in Swedish and Finnish regions with notable seismic activity, although it can have a small influence on modeled heat flow values of Kuusamo, close to the Russian border.

3 EARTHQUAKE DATA

The Institute of Seismology of the University of Helsinki maintains the catalogue of earthquakes recorded by the 24 stations of the Finnish seismograph network (http://www.helsinki.fi/geo/seismo/maanjaristykset/suomi.html). All data are readily available as a table with information about latitude, longitude, focal depth and magnitude. In Sweden, earthquake data are registered by 65 stations and gathered by the University of Uppsala. The Swedish-language site of the Swedish seismograph network provides a Google map application (http://snsn.geofys.uu.se/map/map.php) which can be used to fetch earthquake data registered since year 2000. For further analysis, we imported latitude, longitude, focal depth and magnitude information of events to Python scripts, and combined these data to those obtained in Finland.

In our analysis, all observations from the Finnish and Swedish earthquake catalogues of years 2000–2015 were used, except for data with magnitudes less than 0.1, and for a few events with locations far outside both Swedish and Finnish territory (for example in the Norwegian Sea, Skagerrak or Russian Karelia). One event also had an obviously incorrect depth (125.6 km) and was

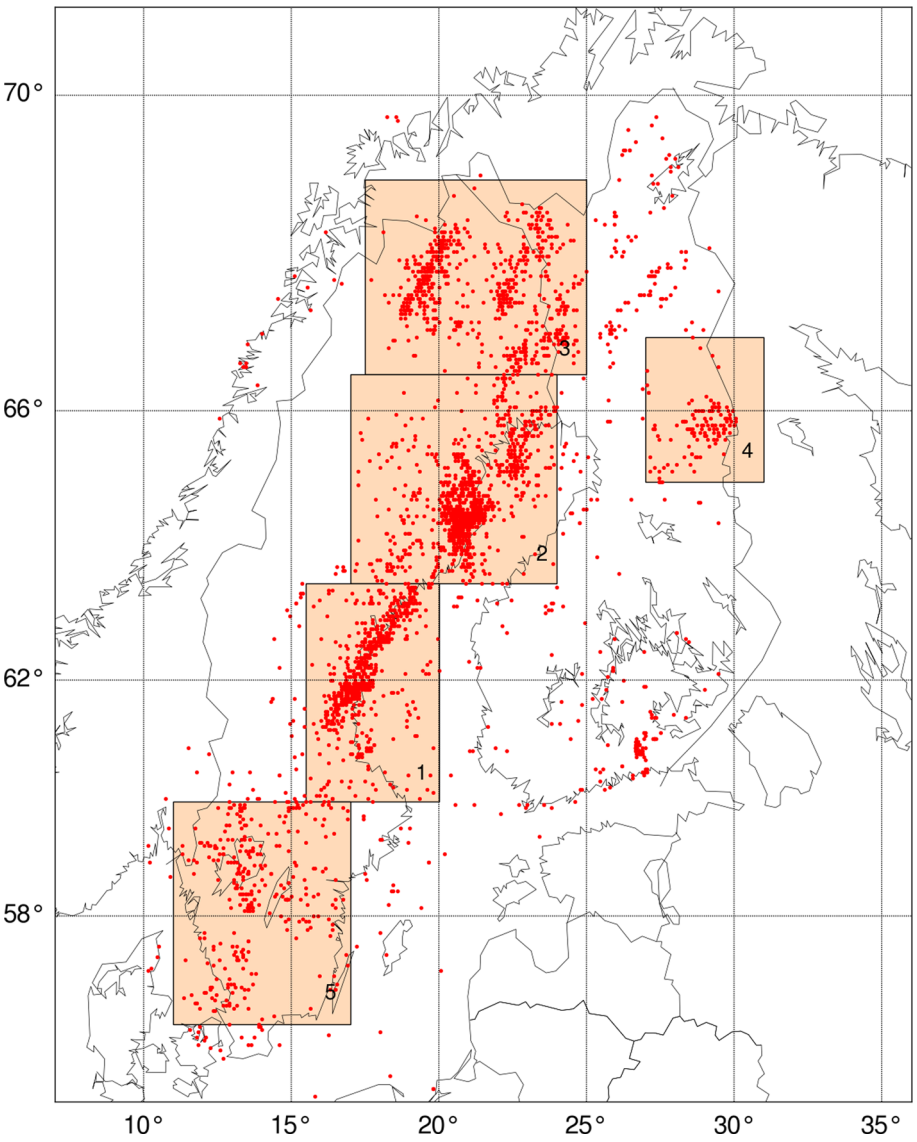

Figure 2. Spatial distribution of all earthquakes (4190 events) accepted for our analysis. Magnitude or depth data are not shown. Area of this map is similar to that of the heat flow map. The rectangles, numbered by '1', '2', '3', '4' and '5' indicate regions where the heat flow field and earthquakes were taken into more detailed investigations (southern Gulf of Bothnia, northern Gulf of Bothnia, Norrbotten/Lapland, Kuusamo region and southern Sweden) as explained in the 'Earthquake data' section of the text. Data from Appendix B.

therefore dismissed. It turned out that a small minority of observations, particularly in the Swedish catalogue, had focal coordinates outside the country, typically in Danish or Norwegian territory close to the Swedish border. However, in this paper observations obtained from Swedish network are simply referred to as Swedish data, and those from Finnish network as Finnish data. Especially in the Gulf of Bothnia and in the proximity of the land border between Finland and Sweden, some earthquakes had been registered by both Finnish and Swedish stations. Although a qualitative visual comparison of epicentral latitudes and longitudes of Finnish and Swedish earthquakes proved that the duplicate problem cannot produce a strong bias to results, we used the event time, latitude, longitude and magnitude data to filter out all obvious duplicates. Altogether 66 events were removed as being duplicates, and 15 events for other reasons as explained in Appendix B. Both in Finland and Sweden, catalogued earthquake magnitudes are local magnitudes (M_L) which closely correspond to the original Richter magnitude but have been determined using a modified function better suited for modern seismometers (Valtonen *et al.* 2013).

In total, 801 Finnish and 3389 Swedish values were accepted for analysis (Fig. 2, Appendix B). Therefore, only 1.9 per cent of data required removal. In the Finnish data, remarkable clusters of earthquakes are visible in the Kuusamo–Kandalaksha zone, and the Bothnian Bay shear zone in western Lapland (Uski *et al.* 2012), and events with depths greater than 25 km are almost exclusively limited to these areas (Fig. 3). The data of northern Sweden show a high spatial frequency of deep earthquakes around the glacially induced Skellefteå fault compared to that associated with other faults such as Lansjärv and Pärvie (Juhlin *et al.* 2010) which otherwise show remarkable seismic activity. The Umeå-Skellefteå area also experiences the most rapid land uplift rate in Fennoscandia, as much as 8 mm yr^{-1} (Steffen & Wu 2011). The uplift rate in Ostrobothnia, on the opposite shore, is nearly as large, but earthquake activity is low perhaps due to the lack of intraplate fault lines. Hence, the glacial isostatic adjustment alone cannot explain the large number

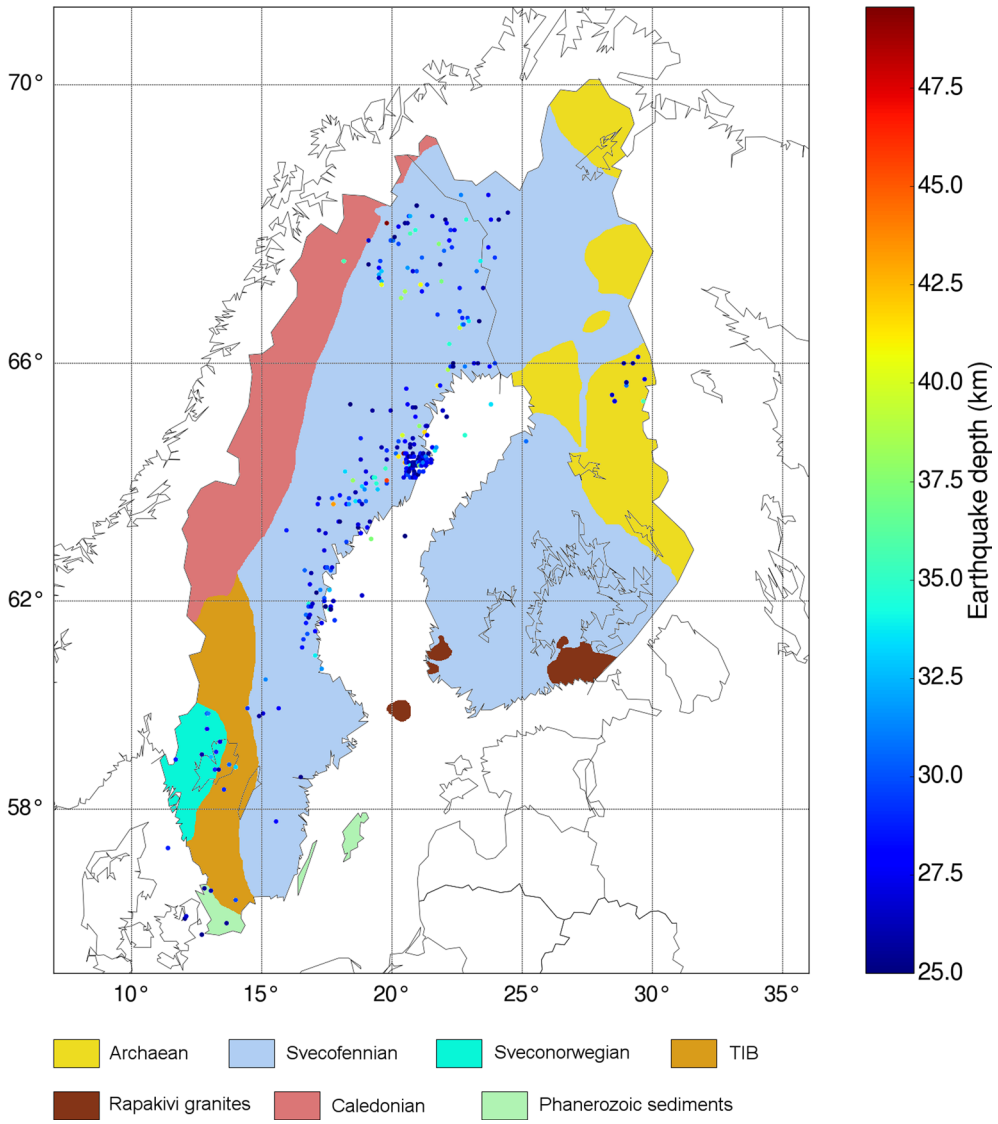

Figure 3. Spatial distribution of deep earthquakes (focal depth at least 25 km) from Finnish and Swedish data sets. Colour bar indicates the focal depth. The total count of data is 317. Latitude–longitude limits of the map are same as those in Figs 1 and 2. Schematic geological units within Finland and Sweden are also shown. TIB refers to Trans-Scandinavian Igneous Belt.

of seismic events in eastern Sweden (e.g. Muir-Wood 2000; Lund 2005), but the strength of the lithosphere and friction of the faults must also play a notable role in general (Scholz 1998).

Close to the southern part of the Swedish coast of the Bothnian Bay, the Bollnäs fault (Malehmir *et al.* 2015) is a good example of a small, recently discovered glacially induced fault with deep seismicity in a narrow zone. Although no obvious intraplate faults are present in more southern areas of Sweden, the Protogine Zone (Berglund *et al.* 1992) shows an obvious concentration of earthquakes. In the far northern part of the country, deep earthquakes are prominent and they have a relatively even spatial distribution in a large area. Although in our Swedish data no earthquake has a magnitude greater than 5.2, and just 26 events exceed the magnitude of 3.0, there is evidence of palaeoearthquakes up to the magnitude of 8 which plausibly occurred in the time of more rapid glacial isostatic adjustment at the end of the Weichselian glaciation about 9000 yr ago (Arvidsson 1996; Lagerbäck & Sundh 2008).

The depth information is given in both Finnish and Swedish earthquake catalogues with a resolution of 0.1 km, although the actual accuracy of focal depth determination varies depending on the crustal velocity model applied and on the spatial distribution of seismographs. These can cause focal depth estimation errors of 30 per cent or more (Ahjos & Uski 1992). Although all seismographs cannot be analysed separately in a database-wide study, biases are more likely to average out in larger data sets like ours, than in smaller ones. Generally, the Finnish earthquake events appear shallow, with a mean depth of 7.0 km. In our Swedish data, the corresponding value is larger (13.1 km) and close to that of several major earthquake areas in the world (Maggi *et al.* 2000). In Finnish data, linear Pearson correlation coefficient of depth versus magnitude data is very low ($R^2 = 0.0407$). If depth (z) is expressed in kilometres, the linear fit to magnitude data follows the equation $M(z) = 0.0163\ z + 0.879$. In Swedish data, depth is negatively correlated to magnitude and the linear fit equation is $M(z) = -0.0120\ z + 0.975$. To check the validity of our null hypothesis (i.e. magnitude is independent of depth), we applied Student's t-test. Because in the case of Finnish data, the two-tailed critical value in the test is at 95 per cent confidence level larger ($c = 0.0693$) than R^2, there is no reason to

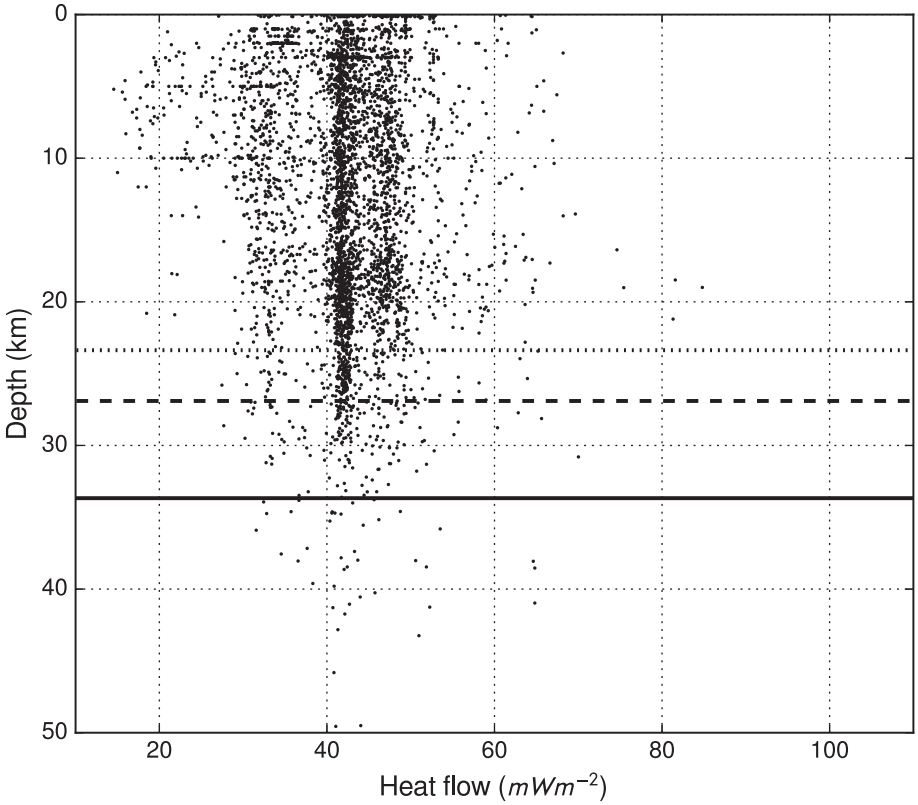

Figure 4. Palaeoclimatically corrected heat flow compared with the earthquake focal depth in all Finnish and Swedish data, except for those with the focal depth less than 0.1 km. Horizontal lines indicate percentiles of focal depths as listed in Table 2. Dotted line refers to the 90th percentile, dashed line to the 95th percentile and solid line to the 99th percentile. Mean surface heat flow at the earthquake epicentres is 49.8 mW m^{-2} and the number of data points is 4190.

reject the null hypothesis. For Swedish data, $R^2 = 0.0252$, yet the critical value is 0.0337. Therefore, the null hypothesis remains in force also in the Swedish case.

For the purpose of comparison, latitude–longitude coordinates of all earthquake epicentres were assigned surface heat flow values from our interpolated heat flow grid. Hence, we were able to study the dependence of focal depth on the modeled surface heat flow. As seen in Fig. 4, highest occurrence of earthquakes is obtained in regions with corrected heat flow in the range of 48–60 mW m^{-2}. Cut-off depths of seismicity had a range from 23.4 km for the 90th percentile to 33.7 km for the 99th percentile (Table 1). As derived from our interpolated heat flow map (Fig. 1), the corrected mean heat flow at earthquake epicentres turned out to be 49.8 mW m^{-2}, virtually same as the value of 49.7 $\pm$ 0.4 mW m^{-2} obtained by Kukkonen & Jõeleht (2003) as a steady-state heat flow estimate for Fennoscandian Shield and East European Platform at depths of 2000 m and more. Therefore, it is unlikely that earthquake epicentres are strongly biased towards certain lithologies, but they represent the average Fennoscandian crust reasonably well for modeling purposes, and our interpolation works adequately.

To investigate the depth distribution of earthquakes further, we performed separate studies on subsets of two Swedish regions on the coast of the Gulf of Bothnia: first in the southern region, ranging from 60.0° to 63.5°N and 15.5° to 20.0°E (area 1 in Fig. 2) and then in the northern region, ranging from 63.5° to 66.5°N and 17.0° to 24.0°E (area 2 in Fig. 2). Our basal earthquake depth estimate for both regions was derived by calculating both the 90th (Doser & Kanamori 1986) and the 95th and 99th percentiles of focal depths (Magistrale 2002). The 95th percentile turned out to be 26.6 km in the southern subset and 27.5 km in the northern subset (Table 1) where the corrected heat flow is lower, 50.8 mW m^{-2} compared to 55.7 mW m^{-2} in the southern subset (Fig. 5). The mean depth of events is 13.0 and 14.3 km, respectively. These two subsets included more than half (804 + 1489 = 2293, 54.7 per cent) of all data.

In addition to studying Swedish coastal regions with high concentrations of earthquakes, we also investigated the Swedish Norrbotten and western Finnish Lapland with more scattered earthquake locations (area 3 in Fig. 2, from 66.5° to 69.0°N and 17.5° to 25.0°E). In area 3, the total number of 864 earthquakes appeared to be concentrated on two distinct heat flow regions, which very roughly represented the older lithosphere with low heat flow and the younger lithosphere with high heat flow. However, the scatter of data in latitude–longitude dimensions was obviously larger than in cases of areas 1 and 2. In area 3, the seismic cut-off depth was 27.8 km (95th percentile) and the mean depth of seismic events was 10.6 km. The palaeoclimatically corrected mean heat flow was 45.0 mW m^{-2} (Fig. 5).

Except for the western Lapland and the Kuusamo region, no other large concentrations of seismic events are located in the Finnish territory. In the Kuusamo region (area 4 in Fig. 2, from 65.0° to 67.0°N and 27.0° to 31.0°E), the total number of events appeared to be 139, palaeoclimatically corrected heat flow 34.9 mW m^{-2}, basal earthquake depth 24.0 km and mean earthquake depth 15.1 km. Excluding Scania, southern Sweden (area 5 in Fig. 2, from 56.0° to 60.0°N and 11.0° to 17.0°E) had a high corrected heat flow (61.9 mW m^{-2}), but the mean depth of the total of 323 earthquake events in the area (14.2 km) and the cut-off depths resembled those of other regions.

The five regional subsets of data used in our analysis incorporate 3619 observations, 86.3 per cent of all earthquake events in Finnish

Table 1. Earthquake cut-off depths (km) corresponding to the 90th, 95th and 99th percentiles of data in our five subsets and mean values weighted using the number of data in each subset as a weight.

	1 ($N = 804$)	2 ($N = 1489$)	3 ($N = 864$)	4 ($N = 139$)	5 ($N = 323$)	Entire area ($N = 4265$)	Weighted mean
90th	22.4	25.1	21.9	24.0	22.8	23.4	23.5 ± 1.4
95th	26.6	27.5	27.8	26.3	27.1	26.9	27.3 ± 0.5
99th	30.4	34.7	35.6	(31.1)	(31.1)	33.7	33.5 ± 2.1

Notes: Values for the entire study area of this paper, not limited to the five subsets, are also given. Parentheses indicate that less than five events with a greater focal depth than the cut-off depth have been registered in the area.

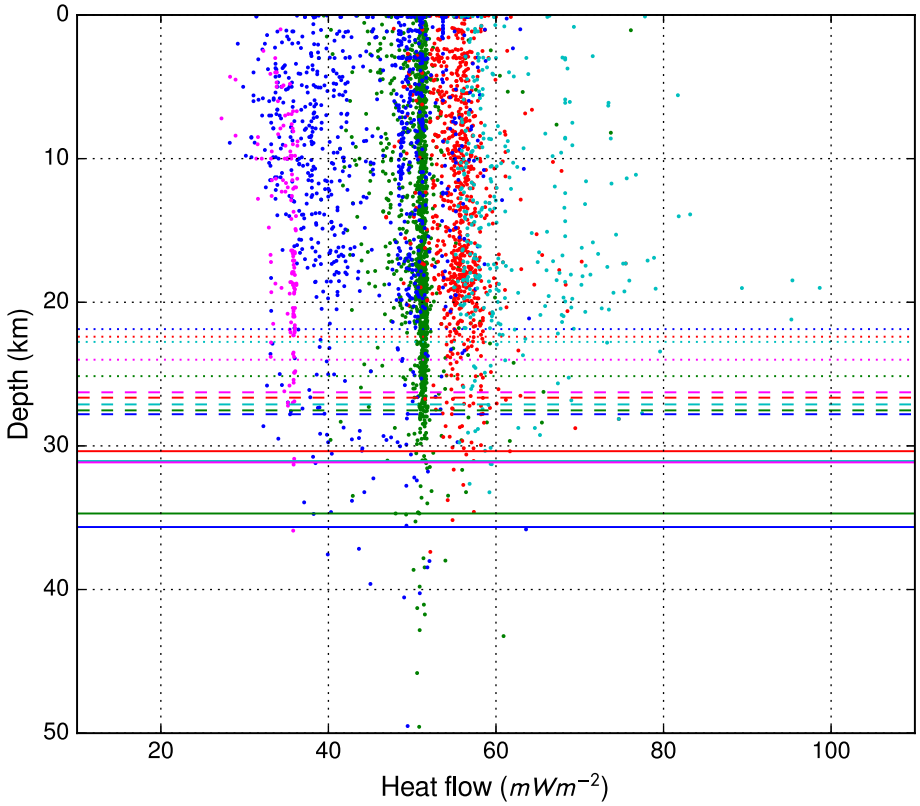

Figure 5. Palaeoclimatically corrected heat flow compared with the earthquake focal depth in five subsets of data: southern Gulf of Bothnia (area 1; red dots), northern Gulf of Bothnia (area 2; green dots), Norrbotten/Lapland (area 3; blue dots), Kuusamo (area 4; pink dots) and southern Sweden (area 5; cyan dots). Dotted lines, dashed lines and solid lines indicate the 90th, 95th and 99th percentiles of focal depths for all subsets, respectively. For interpretation of references to colour in this figure caption, the reader is referred to the online version of the paper.

and Swedish data sets combined. By weighting the obtained cut-off depths by the number of observations in these subsets, a mean estimate and standard deviations for the cut-off depth were calculated, being 23.5 ± 1.4 km for the 90th percentile, 27.3 ± 0.5 km for the 95th percentile and 33.5 ± 2.1 km for the 99th percentile of focal depths. The arithmetic mean of these values is 28.0 km and the standard deviation is 4.1 km. Using all 4190 earthquake events, including but not limited to all five subsets, results in cut-off depths which are within the standard deviations of data calculated from subsets only. As calculated from all 4190 events, the arithmetic mean cut-off depth was 28.0 km with a standard deviation of 4.3 km. The value of 31 km determined for the 99th percentile of focal depths by Kaikkonen *et al.* (2000), using Finnish data only, is therefore slightly smaller than our corresponding value of Finland and Sweden combined. Kaikkonen *et al.* (2000) also concluded that the wet crustal model for brittle-ductile transition works better than the dry one for the Finnish crust, although their assumed depth ranges for the frictional transition temperature of 350 °C is large (25–44 km). Despite the fact that a variety of lithologies in Fennoscandia, from granitic to ultramafic rocks, is represented in the range of epicentral coordinates, our data indicate no obvious relationship between heat flow and seismic cut-off depth. Our smallest data sets, namely those of areas 4 and 5, produce results relatively similar to those of the three larger data sets. Therefore, the entire range of seismogenic zone appears to be relatively well constrained also in the smaller data sets, and we suggest that 28 ± 4 km can be applied to approximate the depth of 350 °C isotherm in general models of the Fennoscandian lithosphere. The temperature corresponds to the change from elastic-brittle deformation to crystal plasticity of quartz, the rheologically weakest major rock-forming mineral in the crust (Scholz 1998).

Fig. 6 shows the depth histograms for all subsets in our study. Mean depths of seismic events within subsets range from 10.6 km in northern Sweden to 15.1 km in Kuusamo region, a variation almost similar to that observed in the cut-off depth. The large number of shallow events in northern Sweden is attributed to the plentiful small immature fault zones, while the seismic activity in areas 1 and 2 is concentrated on a smaller number of well-developed faults, leading

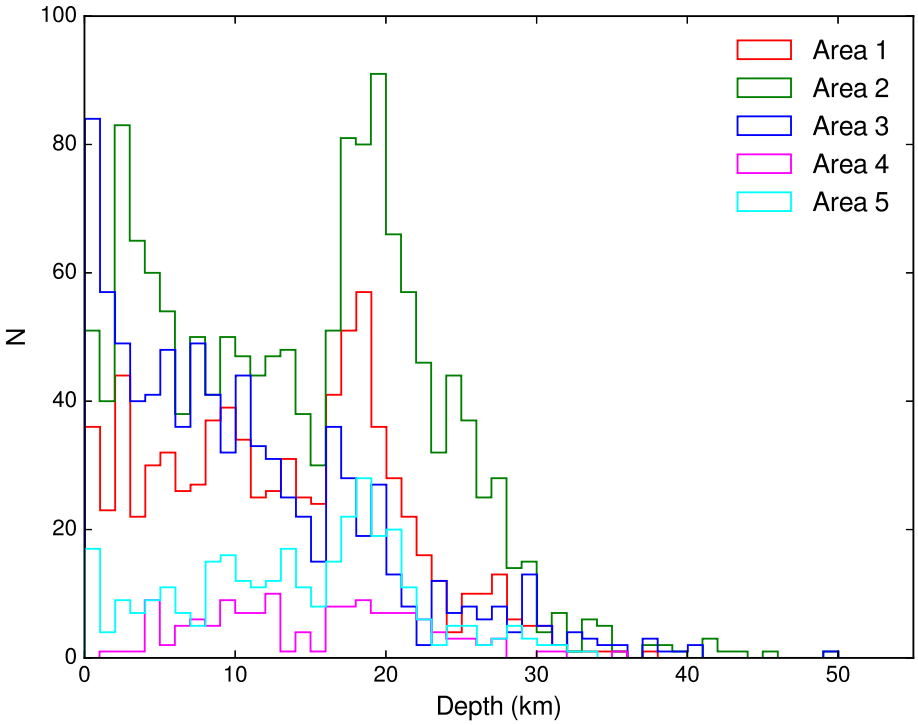

Figure 6. Depth histograms of earthquakes in our subsets of data: southern Gulf of Bothnia subset (area 1), northern Gulf of Bothnia subset (area 2), Norrbotten/Lapland subset (area 3), Kuusamo subset (area 4) and southern Swedish subset (area 5).

to deeper earthquakes. All histograms exhibit a peak at the depth of 15–25 km, a depth where the earthquake mechanism transforms from slick slip to stable sliding, at temperatures of 200–300 °C (Ranalli 1995).

4 THERMAL MODELS AND THEIR RESULTS

Attempts to give isotherm depth estimates for Precambrian areas using heat flow data or spectral analysis of magnetic sources suffer from the non-uniqueness of methods applied, and from the approximate nature of various parameters used in the models. Fortuitously, Moho depth can be credibly estimated using structural seismology (Kinck *et al.* 1993; Grad *et al.* 2009, 2014; Silvennoinen *et al.* 2014), and in addition to seismic cut-off depth, serves as a useful thermal boundary in models if its temperature or heat flow is known. On the crust, heat flow is highly affected by near-surface sources due to strong differentiation of radiogenic heat sources in the crust with high heat production values in felsic upper crustal rock types and low values in mafic lower crustal rock types. In their analysis of Finland only, Kukkonen & Järvimäki (1991) applied Moho depths from seismic wide-angle surveys and estimated Moho heat flow values using a layer model and surface heat flow determinations available. Heat production was approximated with the heat production versus seismic P velocity (A–V_P) relationship (Rybach & Buntebarth 1984). Their range of Moho heat flow was 16.7–37.3 mW m^{-2} with a mean of 21.9 mW m^{-2}. Using superdeep boreholes only, Kremenetsky *et al.* (1989) suggested that heat flow from the mantle is 22–24 mW m^{-2}. A–V_P relationships have been shown to be only approximate, and to provide only trends which cannot be used for detailed estimation of crustal heat production (e.g. Kukkonen & Peltoniemi 1998; Kukkonen & Lahtinen 2001). More robust estimates based on geothermobarometry of mantle xenoliths in eastern Finland have provided much lower values, 12 ± 3mW m^{-2} (Kukkonen & Peltonen 1999; Kukkonen & Lahtinen 2001; Kukkonen *et al.* 2003). These are not derived from crustal heat flow and heat production constraints, thus providing independent estimates for geotherms and mantle heat flow estimation. For other Precambrian regions, such as Trans-Hudson orogen and Slave and Kalahari cratons, xenolith-based mantle heat flow estimates are also available, and their values are in the range of 12–25 mW m^{-2} (Mareschal & Jaupart 2013).

For central Fennoscandia, Jokinen & Kukkonen (1999a,b) and Kukkonen *et al.* (1999) applied a generic model for uncertainty analysis of forward and inverse geotherm calculations. They used a model with a 50 km thick crust composed of three layers with constant (temperature-independent) thermal conductivities and heat productions as follows: 3.00 Wm^{-1}K^{-1} and 1.8 μW m^{-3} (0–10 km; layer 1), 2.75 Wm^{-1}K^{-1} and 0.6 μW m^{-3} (10–30 km; layer 2) and 2.50 Wm^{-1}K^{-1} and 0.2 μW m^{-3} (30–50 km; layer 3). Our forward modeling partly followed the same guidelines, although we applied a temperature-dependent continuous function to represent thermal conductivity (Cermak & Haenel 1988; eqs 1 and 2) and we also required that the 350 °C isotherm stays within the seismic cut-off depth range of 28 ± 4 km. Our models consisted of three crustal layers (upper, middle and lower layers) and an upper-mantle layer. The upper crustal layer (layer 1) was fixed at 0–10 km, while the depth of 28 km represented the boundary of middle (layer 2) and lower (layer 3) crust. As surface conditions in all models, we applied a steady-state heat flow value (corresponding to the palaeoclimatically corrected heat flow). Our three models had different surface heat flow values (40, 50 and 60 mW m^{-2}) and upper crustal heat production constraints (1.1, 3.3 and 2.1 μW m^{-3}), respectively. In all models, thermal conductivity at the surface was 2.70 Wm^{-1}K^{-1} and temperature was $T_0 = 3$ °C, which represents the annual mean ground surface temperature in the study area. In addition, we applied the average Moho depth of Fennoscandia, namely 46 km

Table 2. Temperature and heat flow at layer boundaries in our models.

	Temperature (°C)			Heat flow (mW m^{-2})			Thermal conductivity (Wm^{-1}K^{-1})		
	Model 1	Model 2	Model 3	Model 1	Model 2	Model 3	Model 1	Model 2	Model 3
Surface (0 km)	3	3	3	50	40	60	2.70	2.70	2.70
Boundary of layers 1 and 2 (10 km)	159	138	175	29.0	29.0	27.0	2.40	2.43	2.37
Boundary of layers 2 and 3 (28 km)	348	324	349	18.2	18.2	16.2	2.11	2.14	2.11
Moho (46 km)	494	468	477	14.6	14.6	12.6	2.62	2.62	2.62
LAB (250 km)	1583	1557	1410	14.2	14.2	12.2	2.62	2.62	2.62

Notes: Heat production was kept constant within each layer as explained in Section 4 of the text. Thermal conductivity was a continuous function of temperature in the crust, but constant in the mantle (between Moho and LAB). For corresponding geotherms, see Fig. 7.

(Grad *et al.* 2014) as the fixed lower boundary of the crust in all models, above the mantle part of the lithosphere which was assumed to have its lower boundary at the depth of 250 km.

In order to correct for the temperature dependence of thermal conductivity, various empirical relations have been published, yet all of them are strongly bound to the assumed lithology, which is far from uniform. They typically become less functional in high temperatures (Lee & Deming 1998; Vosteen & Schellschmidt 2003). Generally, thermal conductivity (λ) can be described by the equation

$$\lambda = \lambda_0 \left[1/(1 + bT) + c(T + 273.15K)^3\right] \quad (1)$$

where λ_0 is the value at the reference temperature of 25 °C (2.7 Wm^{-1}K^{-1} applied here) and b (0.0008 1/K) is a pre-selected empirical parameter, depending on lithology but typically being close to the value of 0.001 1/K in crust. The factor c represents radiative heat transfer, which is not significant at temperatures below 800 °C (Kukkonen & Peltonen 1999) and is therefore neglected in the crustal part of our modeling. The steady-state temperature T at a given depth z from the upper boundary of the layer was solved using eq. (2)

$$T(z) = (1/b)\left\{(1 + bT_0)\exp\left[\left(\frac{b}{\lambda_0}\right)\left(q_0 z - \frac{Hz^2}{2}\right)\right] - 1\right\} \quad (2)$$

where H is heat production in the layer, assumed constant. It is conceivable that radiogenic heat production shows the highest values and variations in the upper crust, whereas middle and lower crusts have much smaller and more stable values. It is supported by global observational data that surface heat production and heat flow are correlated in continental areas (e.g. Jaupart & Mareschal 2003). Therefore, to find representative generic geotherms for different heat flow areas we kept the middle and lower crustal heat production values (0.6 and 0.2 μW m^{-3}) unchanged in the model, but varied the upper crustal heat production values to produce variation in surface heat flow. The geotherms were required to be in agreement with the seismic cut-off temperature of 350 °C at the depth of 28 ± 4 km and with the representative heat flow of 9–15 mW m^{-2} at Moho and in the mantle lithosphere. Moreover, we demanded that mantle temperature did not exceed 1500–1600 °C at the base of the lithosphere (250 km), in line with Fennoscandian mantle xenolith pressure–temperature data (Kukkonen & Peltonen 1999; Kukkonen *et al.* 2003). Mantle heat production was assigned a very small value (0.002 μW m^{-3}).

Our mantle conductivity was calculated by approximating the decreasing phonon conduction and increasing radiative heat transfer in the typical subcrustal temperature range of 500–1500 °C, using eq. (1), but with parameters different from those used in the crust. Values of λ_0 (4.0 Wm^{-1}K^{-1}), b (0.0015 1/K) and c (10^{-10} 1/K^3) were based on ultramafic lithology and olivine heat transfer data (Schatz & Simmons 1972; Zoth & Haenel 1988). The average $\lambda(T)$ in the desired range turned out to be 2.62 Wm^{-1}K^{-1}, and the mantle conductivity was kept at this constant value in the calculations.

In the crust, a reasonable fit with the temperature of the earthquake cut-off depth (24–32 km) was used as the primary criterion for accepting the geotherms. Temperature data from deep boreholes were also used as guiding information in the upper crust. We applied the value of 130 °C measured at 8 km in the Kola super-deep hole after 559 d of shut-in time (Popov *et al.* 1999), and the value of 40 °C at 2.5 km measured at the bottom of the Outokumpu deep drill hole (Kukkonen *et al.* 2011). The values applied in the models are shown in Table 2, and the corresponding geotherms in Fig. 7.

The resulting geotherms representing surface heat flow values 40–60 mW m^{-2} are all in agreement with the earthquake cut-off depth temperature, and the mantle heat flow implied by xenolith thermobarometry. The Moho temperatures are in the range of 460–500 °C. They also allow very thick thermal lithosphere thickness of 200–250 km, in agreement with seismic estimates (Plomerová & Babuška 2010). With (steady-state) surface heat flow values lower than 40 mW m^{-2}, it turned out to be very difficult to fulfill the desired thermal and rheological criteria. This limitation originates from the typical values of heat production in rocks (e.g. Rybach 1988), which together with crustal thickness and mantle heat flow set a minimum level for the surface heat flow value. It is possible that such low heat flow values are not representative of the Fennoscandian crust.

5 DISCUSSION

Constructing steady-state geotherms for an area the size of Finland and Sweden combined involves a number of uncertainties affecting temperature and heat flow estimates at Moho, at other boundaries and between. Among the initial values applied, the mean ground surface temperature is known best, yet small changes in its value have little influence on temperatures in the deeper crust. The lowest (near) surface heat flow values, for example that of Sodankylä (palaeoclimatically uncorrected value 12.7 mW m^{-2}; Appendix A; Kukkonen 1989a) most probably reflect poorly controlled palaeoclimatic history of the site. Central Lapland was under the ice divide during the Late Weichselian glaciation, which may have resulted in downward advecting ice and very low temperatures at the bottom of the glacier. Unfortunately, values of palaeoclimatic corrections in parts of Fennoscandia can be of same magnitude, or even larger than the uncorrected result itself, which is therefore seriously compromised. As an extreme example, Demezhko *et al.* (2013) analysed temperature data in a 3.3 km deep hole in the Onega Lake area, Russian Karelia, and inverted the data for palaeotemperatures. The results suggest a steep temperature increase of 18–20 °C at the Weichselian/Holocene transition.

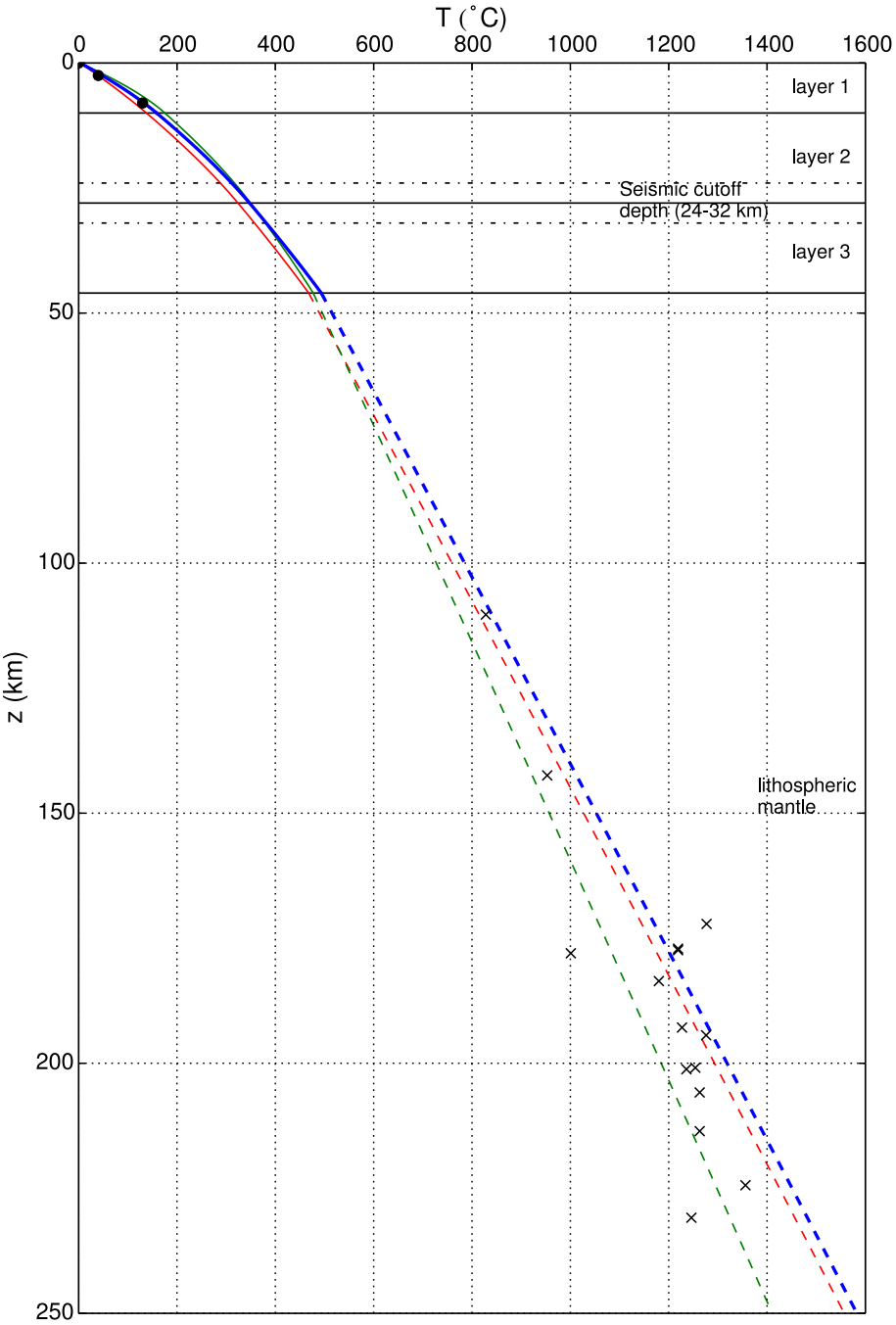

Figure 7. Geotherms of the Fennoscandian lithosphere, featuring temperature-dependent thermal conductivity and fixed heat production constraints for crustal layers 1, 2 and 3. In the mantle, both conductivity and heat production were fixed. Model 1 (surface heat flow 50 mW m^{-2}) is represented by the blue curve, model 2 (40 mW m^{-2}) by the red curve and model 3 (60 mW m^{-2}) by the green curve. Circle symbols indicate the temperature of Kola superdeep borehole at 8 km and Outokumpu borehole at 2.5 km depth, and cross symbols indicate xenolith thermobarometric data in the lithospheric mantle in Fennoscandian Shield. For numeric values used in models, see Section 4 and Table 2.

Crustal heat production is also rather poorly known thermal parameter. It depends on the estimated concentrations of uranium (U), thorium (Th) and potassium (K), which are more abundant in accessory minerals than in main constituents of typical rocks (Jaupart & Mareschal 2003). In the Finnish rock geochemical database (Rasilainen *et al.* 2007), 6526 outcrops give a value of 1.33 $\pm$ 1.19 μW m^{-3}, yet this is valid only in the immediate vicinity of surface, a problem typical of regional and global compilations. For Sweden, no corresponding data compilation has been published, but given the higher proportion of Proterozoic granitic rocks in the Swedish than in the Finnish lithosphere, we can assume the near-surface heat production in Sweden to be perhaps 0–20 per cent larger, although local variations are great. For example, the Sveconorwegian Bohus granite area features five-fold changes in thorium concentrations in scales ranging from tens of metres to kilometres (Landström *et al.* 1980). In general, near-surface heat production is more strongly dependent on rock type rather than on depth, and no obvious trend is visible

in superdeep holes (e.g. Kremenentsky *et al.* 1989; Clauser *et al.* 1997).

Previous global estimates of the thickness of the upper crustal heat producing layer range from 2 km to as much 16 km (Hasterok & Chapman 2011). Although simplistic models of linear heat flow–heat production relationship (Artemieva & Mooney 2001) suggest the heat producing layer, the 'upper crust', to be 8–10 km thick, this value, also referred to as 'depth parameter', is not related to any physical boundary. For Fennoscandian middle and lower crust, precise heat production constraints are not available, and for the time being, our method of using approximate values which fulfill boundary conditions is the only way to proceed. However, for southern Africa, Michaut *et al.* (2007) calculated a xenoliths-based heat production constraint of 0.34 ± 0.08 μW m^{-3}, corresponding to the depth range of 10–35 km. It appears that when heat production constraints in layers 2 (10–28 km) and 3 (28–46 km) of our models (0.6 and 0.2 μWm^{-3}) are weighted by depths of 18 and 7 km, we get a value of 0.49 μW m^{-3}, which is close to the southern African estimate. However, the Moho heat flow, as determined from xenolith thermobarometry, is much larger (17–25 mW m^{-2}, Rudnick & Nyblade 1999) in southern Africa than in Fennoscandia, thus implying different conditions in the lithospheric mantle and asthenosphere.

Mantle heat flow has been directly determined from kimberlite-hosted mantle xenoliths (Kukkonen & Peltonen 1999; Kukkonen *et al.* 2003), which provide an important lower boundary condition for geotherm calculations. The xenolith-based value is probably representative in a much larger area than the Eastern Finland kimberlite province, as suggested by the modeling of the effects of mantle heat flow variations on lithosphere isostasy and lack of major elevation contrasts in most of Finland, eastern Sweden, and NE Russia (Kukkonen 2014). It is conceivable that the thick lithosphere in Fennoscandian Shield in represented by relatively uniform and low-mantle heat flow. For a 250 km thick lithosphere used in our models, the characteristic time of heat diffusion is as much as 2 Ga, meaning that steady-state thermal models should be considered approximate (Michaut *et al.* 2007). In addition, the uncertainty in calculated temperatures increases quickly with depth. Kukkonen *et al.* (1999) carried out an uncertainty analysis for a simple four-layer lithosphere model, and the uncertainty of calculated temperature at 50 km may easily amount to ±150 °C when the geotherm is calculated using the surface heat flow and ground surface temperatures as boundary conditions. The uncertainty can be reduced if independent data on the crustal and mantle temperature and heat flow can be incorporated in the modeling.

The accuracy of the depth estimation of earthquakes depends on various factors, such as the quality of the velocity model, the accuracy of picking the signals, the largest azimuthal gap from event to stations and distance to closest station. Especially, the shortest distance to station which produces a good quality *S* phase pick is a good constraint to earthquake depth. Gomberg *et al.* (1990) defined that to obtain an accurate depth estimate (error < 1.5 km), the closest station with *S* phase pick should lie closer than 1.4 times the depth from the source. In our study, the parameters which affect the accuracy of earthquake depth estimation are rather stable. The velocity models have been almost constant though different at different areas, and the azimuthal coverage of stations is good. The parameter with largest variation is distance to the nearest station. In our study areas 1, 2 and 5, the average distance to the nearest station is estimated to be 30 km. In area 3, the distance is 20 km and in area 4, 25 km, respectively. These estimates give the depths below which the accuracy of earthquake depth is at least 1.5 km. The threshold depth for areas 1, 2 and 5 is 21 km, for area 3, 14 km and for area 4, 18 km, respectively. Above the threshold depths, the accuracy is > 1.5 km, but it varies within study areas. The estimates apply best to sites with largest concentrations of earthquakes. For some smaller regions, independent depth accuracy estimates are available. For a local network in Kalajoki, partly in our area 2, Tiira *et al.* (2016) estimated accuracy of hypocentre depth to be 3–4 km without any analysis of accuracy variation with depth. Similar single value estimates were given by Lindblom (2011) for Pärvie fault in our area 3 (4 km) and by Uski *et al.* (2012) for Kuusamo region in our area 4 (also 4 km). It appears from Fig. 8 that deep earthquakes are rare in areas with corrected heat flow greater than 60 mW m^{-2}. Deepest events (49.6, 49.5, 45.8, 43.2 and 42.8 km) are not situated in areas with smallest palaeoclimatically corrected heat flow (less than 48 mW m^{-2}), and their locations are very scattered in general. A visual inspection of FennoscandianMoho depth maps (Grad *et al.* 2009, 2014) is enough to reveal their closeness to Moho.

Results presented in this paper are heavily dependent on the representativeness of the assumed 350 °C temperature at the seismic cut-off depth. The cut-off temperature depends on the rheology of the rocks, which is mainly controlled by mineral composition and presence of volatiles. Traditionally, the crustal strength and rheological behaviour has been seen as a question whether the rocks are brittle or ductile. According to this view, the prevailing deformation mechanism simply depends on which of the mechanisms provides the smaller yield strength value. This model implies that earthquakes may occur down to the base of the brittle layer. The brittle behaviour is described by Byerlee's law (Brace & Byerlee 1966) which is not dependent on rock type, but rather on vertical stress, type of faulting, friction and pore pressure. The ductile rheology which typically follows a power-law function is strongly affected by the rock composition and temperature. In quartz-bearing rocks, the brittle-ductile transition takes place at about 350 °C, but if the rock is more mafic the transition is at higher temperatures, and the rheologically important minerals are feldspar or amphiboles.

Earthquakes are not simply controlled by the brittle-ductile transition of a homogeneous medium. Instead, they usually occur in pre-existing faults or zones of weakness. Slipping of the fault is controlled by the frictional stability of the fault. Frictional stability defines the conditions where earthquakes occur. In granitic (quartz-rich) rocks, this takes place at temperatures below *ca.* 300–350 °C. Above this temperature, the fault is in a stable regime where the yield is continuous. On the other hand, at low temperatures, the fault may also be in a stable regime due to flow in a cataclastic or poorly consolidated material. If the fault has a poorly developed gauge (e.g. recently formed faults), the low-temperature stability may reach close to the surface, but usually extends to depths of some kilometres. Thus, earthquakes occur in the unstable frictional regime of the fault, and may extend in depth from a few kilometres to the depth of the 300–350 °C isotherm (Scholz 1998). Depending on the properties of the frictional properties of the fault, prevailing stress and deformation rates, earthquakes may occur also deeper than the traditional brittle-ductile transition would indicate. Therefore, the seismic cut-off depth is not a sharply defined boundary, but a transition affected by the rock mineral composition and the frictional instability of faults and temperature.

6 CONCLUSIONS

Our result that surface heat flow values and earthquake cut-off depths do not correlate has important implications. Assuming that

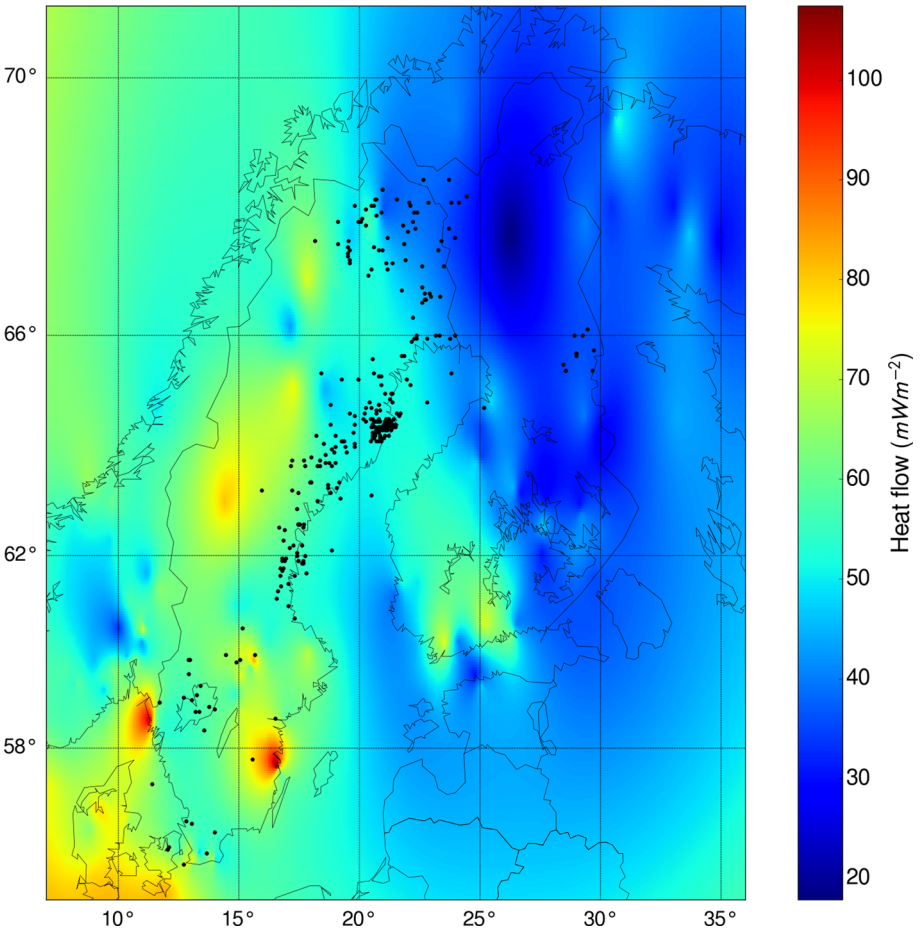

Figure 8. Epicentral locations of deep earthquakes (focal depth over 25 km) on a contour map of palaeoclimatically corrected heat flow (mW m^{-2}).

in the intraplate conditions of Fennoscandian Shield, the earthquake mechanisms represent the same rheological properties in different areas, the crustal temperature must be relatively uniform at the cut-off depth. Then, the observed surface heat flow variations must be due to variations in radiogenic heat production in the crust, and particularly in the upper crust. U, Th and K are strongly differentiated in geological processes, particularly in partial melting. Melting processes have transported and concentrated heat producing elements in the upper crust, and depleted the middle and lower crustal layers. On the other hand, mantle heat flow has been directly determined from kimberlite-hosted mantle xenoliths, which provide an important lower boundary condition for geotherm calculations. Moreover, the xenolith-based mantle heat flow is probably representative in a much larger area than the Eastern Finland kimberlite province, as has been suggested by the modeling of the effects of mantle heat flow variations on lithosphere isostasy and lack of elevation contrasts in most of Finland, eastern Sweden, and northeastern Russia. It is conceivable that the thick lithosphere in Fennoscandian Shield is represented by relatively uniform and low-mantle heat flow.

ACKNOWLEDGEMENTS

Toni Veikkolainen acknowledges funding from the Jenny and Antti Wihuri Foundation, Finland. We thank Kari Moisio and an anonymous reviewer for their helpful comments which improved the manuscript.

REFERENCES

Ahjos, T. & Uski, M., 1992. Earthquakes in northern Europe in 1375–1989, *Tectonophysics,* **207,** 1–23.

Artemieva, I. & Mooney, W., 2001. Thermal thickness and evolution of Precambrian lithosphere: a global study, *J. geophys. Res.,* **106,** 16 387–16 414.

Arvidsson, R., 1996. Fennoscandian Earthquakes: whole crustal rupturing related to postglacial rebound, *Science,* **274,** 744–746.

Berglund, J., Larson, S.Å. & Stigh, J., 1992. Features of the Protogine Zone, south central Sweden, *GFF,* **114,** 337–339.

Blanpied, M.L., Lockner, D.A. & Byerlee, J.D., 1991. Fault stability inferred from granite slidingexperiments at hydrothermal conditions, *Geophys. Res. Lett.,* **18,** 609–612.

Bollinger, G.A., Chapman, M.C., Sibol, M.S. & Costain, J.K., 1985. An analysis of earthquake focal depths in the southeastern U.S., *Geophys. Res. Lett.,* **12,** 785–788.

Bonner, J.L., Blackwell, D.D. & Herrin, E.T., 2003. Thermal Constraints for Earthquake Depths in California, *Bull. seism. Soc. Am.,* **93,** 2333–2354.

Bödvarsson, R., Lund, B., Roberts, R. & Slunga, R., 2006. Earthquake activity in Sweden. Study in connection with a proposed nuclear waste repository in Forsmark or Oskarshamn, p. 40, SKB Rapport R-06-07, Swedish Nuclear Fuel and Waste Management Company.

Brace, W.F. & Byerlee, J.D., 1966. Stick-slip as a mechanism for earthquakes, *Science,* **153,** 990–992.

Cermak, V. & Haenel, R., 1988. Geothermal maps, in *Handbook of Terrestrial Heat Flow Density Determination,* pp. 261–300, eds Haenel, R., Rybach, L. & Stegena, L., Kluwer Academic Publishers.

Clauser, C. *et al.*, 1997. The thermal regime of the crystalline continental crust: implications from the KTB, *J. geophys. Res.,* **102,** 18 417–18 441.

Davies, J.H. & Davies, D.R., 2010. Earth's surface heat flux, *Solid Earth,* **1,** 5–24.

Demezhko, D.Yu., Gornostaeva, A.A., Tarkhanov, G.V. & Esikpo, O.A., 2013. 30,000 years of ground surface temperature and heat flux changes in Karelia reconstructed from borehole temperature data, *Bull. Geog.—Phys. Geog. Ser.,* **6,** 7–25.

Doser, D.I. & Kanamori, H., 1986. Depth of seismicity in the Imperial Valley region (1977–1983) and its relationship to heat flow, crustal structure, and the October 15, 1979, earthquake, *J. geophys. Res.,* **91,** 675–688.

Eliasson, T., Eriksson, K.G., Lindquist, G., Malmquist, D. & Parasnis, D., 1991. Catalogue of heat flow density data: Sweden, in *Geothermal Atlas of Europe,* pp. 124–125, eds Hurtig, E., Cermak, V., Hänel, R. & Zui, V., Hermann Haack.

Eriksson, K.G. & Malmqvist, D., 1979. A review of the past and present investigations of heat flow in Sweden, in *Terrestrial Heat Flow in Europe*, pp. 267–277, eds Cermak, V. & Rybach, L., Springer.

Gomberg, J.S., Shedlock, K.M. & Roecker, S.W., 1990. The effect of S-wave arrival times on the accuracyof hypocenter estimation, *Bull. seism. Soc. Am.,* **80,** 1605–1628.

Grad, M., Tiira, T. & ESC Working Group, 2009. The Moho depth map of the European plate, *Geophys. J. Int.,* **176,** 279–292.

Grad, M., Tiira, T., Olsson, S. & Komminaho, K., 2014. Seismic lithosphere-asthenosphere boundary beneath the Baltic Shield, *GFF,* **136,** 581–598.

Hasterok, D & Chapman, D.S., 2011. Heat production and geotherms for the continental lithosphere, *Earth planet. Sci. Lett.,* **307,** 59–70.

Hurter, S. & Hänel, R., 2002. *Atlas of Geothermal Resources in Europe,* Publication EUR 17811, European Commission, p. 92.

Jaupart, C. & Mareschal, J.C., 2003. Constraints on crustal heat production from heat flow data, in *Treatise on Geochemistry*, pp. 65–84, eds Rudnick, R.L., Holland, H.D. & Turekian, K.K., Elsevier.

Juhlin, C., Dehghannejad, M., Lund, B., Malehmir, A. & Pratt, G., 2010. Reflection seismic imaging of the end-glacial Pärvie Fault system, northern Sweden, *J. appl. Geophys.,* **70,** 307–316.

Jõeleht, A. & Kukkonen, I.T., 1996. Heat flow density in Estonia—assessment of palaeoclimatic and hydrogeological effects, *Geophysica,* **32,** 291–317.

Jokinen, J. & Kukkonen, I.T., 1999a. Random modelling of the lithospheric thermal regime: forward simulations applied in uncertainty analysis, *Tectonophysics,* **306,** 277–292.

Jokinen, J. & Kukkonen, I.T., 1999b. Inverse simulation of the lithospheric thermal regime using the Monte Carlo method, *Tectonophysics,* **306,** 293–310.

Kaikkonen, P., Moisio, K. & Heeremans, M., 2000. Thermomechanical lithospheric structure of the central Fennoscandian shield, *Phys. Earth planet. Inter.,* **119,** 209–235.

Kinck, J.J., Husebye, E.S. & Larsson, F.R., 1993. The Moho depth distribution in Fennoscandia and the regional tectonic evolution from Archean to Permian times, *Precambrian Res.,* **64,** 23–51.

Klemperer, S.L., 1987. A relation between continental heat flow and the seismic reflectivity of the lower crust, *J. Geophys.,* **61,** 1–11.

Korja, A., Uski, M., Lund, B., Högdahl, K., Grigull, S. & Nironen, M., 2016. Observations on intraplate seismicity in Central Fennoscandia, in *EGU General Assembly 2016,* 17–22 April 2016, p. 6108.

Kremenentsky, A.A., Milanovsky, S.Y. & Ovchinnikov, L.N., 1989. A heat generation model for the continental crust based on deep drilling in the Baltic Shield, *Tectonophysics,* **159,** 231–246.

Kukkonen, I.T., 1989a. Terrestrial heat flow and radiogenic heat production in Finland, the Central Baltic Shield, *Tectonophysics,* **164,** 219–230.

Kukkonen, I.T., 1989b. Terrestrial heat flow in Finland, the central Fennoscandian Shield, *PhD thesis*, Helsinki University of Technology, Espoo, Finland.

Kukkonen, I.T., 2014. Mantle heat flow in the Fennoscandian Shield, in *Lithosphere 2014—Eighth Symposium on the Structure, Composition and Evolution of the Lithosphere in Finland. Programme and Extended Abstracts*, pp. 51–52, eds Eklund, O., Kukkonen, I.T., Skyttä, P., Sonck-Koota, P., Väisänen, M. & Whipp, D., Institute of Seismology, University of Helsinki.

Kukkonen, I.T. & Clauser, C., 1994. Simulation of heat transfer at the Kola deephole site: implications for advection, heat refraction and paleoclimatic effects, *Geophys. J. Int.,* **116,** 409–420.

Kukkonen, I.T. & Järvimäki, P., 1991. Catalogue of heat flow density data: Finland, in *Geothermal Atlas of Europe*, p. 29, eds Hurtig, E., Cermak, V., Hänel, R. & Zui, V., Hermann Haack.

Kukkonen, I.T. & Jõeleht, A., 2003. Weichselian temperatures from geothermal heat flow data, *J. geophys. Res.,* **108,** 2163, doi:10.1029/2001JB001579.

Kukkonen, I.T. & Lahtinen, R., 2001. Variation of radiogenic heat production rate in 2.8–1.8 Ga old rocks in the central Fennoscandian shield, *Phys. Earth planet. Inter.,* **126,** 279–294.

Kukkonen, I.T. & Peltonen, P., 1999. Xenolith-controlled geotherm for the central Fennoscandian Shield: implications for lithosphere–asthenosphere relations, *Tectonophysics,* **304,** 301–315.

Kukkonen, I.T. & Peltoniemi, S., 1998. Relationships between thermal and other petrophysical properties of rocks in Finland, *Phys. Chem. Earth,* **23,** 341–349.

Kukkonen, I.T., Kinnunen, K. & Peltonen, P., 2003. Mantle xenoliths and thick lithosphere in the Fennoscandian Shield, *Phys. Chem. Earth,* **28,** 349–360.

Kukkonen, I.T., Olesen, O. & Ask, M.V.S., PFDP Working Group, 2010. Postglacial faults in Fennoscandia: targets for scientific drilling, *GFF,* **132,** 71–81.

Kukkonen, I.T., Gosnold, W.D. & Šafanda, J., 1998. Anomalously low heat flow density in eastern Karelia, Baltic shield: a possible palaeoclimatic signature, *Tectonophysics,* **291,** 235–249.

Kukkonen, I.T., Jokinen, J. & Seipold, U., 1999. Temperature and pressure dependencies of thermal transport properties of rocks: implications for uncertainties in thermal lithosphere models and new laboratory measurements of high grade rocks in the central Fennoscandian shield, *Surv. Geophys.,* **20,** 33–59.

Kukkonen, I.T., Rath, V., Kivekäs, L., Šafanda, J. & Čermak, V., 2011. Geothermal studies of the Outokumpu Deep Drill Hole, Finland: vertical variation in heat flow and paleoclimatic implications, *Phys. Earth planet. Inter.,* **188,** 9–25.

Kuusisto, M., Kukkonen, I.T., Heikkinen, P. & Pesonen, L.J., 2006. Lithological interpretation of crustal composition in the Fennoscandian Shield with seismic velocity data, *Tectonophysics,* **420,** 283–299.

Lagerbäck, R. & Sundh, M., 2008. Early Holocene faulting and paleoseismicity in northern Sweden, SGU Research Paper, C836, pp. 80.

Lahtinen, R., 2012. Main geological features of Fennoscandia, *Geol. Surv. Finland Spec. Paper,* **53,** 13–18.

Landström, O., Larson, S.-Å., Lind, G. & Malmqvist, D., 1980, Geothermal investigations in the Bohus granite area in southwestern Sweden, *Tectonophysics,* **64,** 131–162.

Lee, Y. & Deming, D., 1998. Evaluation of thermal conductivity temperature corrections applied in terrestrial heat flow studies, *J. geophys. Res.,* **103,** 2447–2454.

Lehtinen, M., Nurmi, P.A. & Rämö, O.T., 2006. *Precambrian Geology of Finland. Key to the Evolution of the Fennoscandian Shield,* Elsevier, p. 750.

Lindblom, E., 2011. Microearthquake study of end-glacial faults in northern Sweden, *PhLic thesis*, University of Uppsala, Uppsala, Sweden.

Lund, B., 2005. Effects of deglaciation on the crustal stress field and implications for endglacial faulting: a parametric study of simple Earth and ice models. Technical Report, Swedish Nuclear Fuel and Waste Management Co. Stockholm, TR-05-04, p. 68.

Lund, B., Schmidt, P. & Hieronymus, C., 2009. Stress evolution and fault instability during the Weichselian glacial cycle. Technical Report, Swedish Nuclear Fuel and Waste Management Co., Stockholm, TR-09-15, p. 106.

Mackwell, S.J., Zimmerman, M.E. & Kohlstedt, D.L., 1998, High-temperature deformation of dry diabase with application to tectonics on Venus, *J. geophys. Res.,* **103,** 975–984.

Magistrale, H., 2002. Relative contributions of crustal temperature and composition to controlling the depth of earthquakes in Southern California, *Geophys. Res. Lett.,* **29**(10), 1447, doi:10.1029/2001GL014375.

Maggi, A., Jackson, J.A., McKenzie, D. & Priestley, K., 2000. Earthquake focal depths, effective elastic thickness and the strength of the continental lithosphere, *Geology,* **28,** 495–498.

Majorowicz, J. & Wybraniec, S., 2010. New terrestrial heat flow map of Europe after regional paleoclimatic correction application, *Int. J. Earth Sci.,* **100,** 881–887.

Malehmir, A. *et al.*, 2015. Post-glacial reactivation of the Bollnäs fault, central Sweden, *Solid Earth Discuss.,* **7,** 2833–2874.

Mareschal, J.-C. & Jaupart, C., 2013. Radiogenic heat production, thermal regime and evolution of continental crust, *Tectonophysics,* **609,** 524–534.

Michaut, C., Jaupart, C. & Bell, D.R., 2007. Transient geotherms in Archean continental lithosphere: new constraints on thickness and heat production of the subcontinental lithospheric mantle, *J. geophys. Res.,* **112,** B04408, doi:10.1029/2006JB004464.

Moisio, K., 2005. Numerical lithospheric modelling: rheology, stress and deformation in the central Fennoscandian Shield, *PhD thesis*, University of Oulu, Oulu, Finland.

Mottaghy, D., Schellschmidt, R., Popov, Y.A., Clauser, C., Kukkonen, I.T., Nover, G., Milanovsky, S. & Romushkevich, R.A., 2005. New heat flow data from the immediate vicinity of the Kola super-deep borehole: vertical variation in heat flow confirmed and attributed to advection, *Tectonophysics,* **401,** 119–142.

Muir-Wood, R., 2000. Deglaciation seismotectonics: a principal influence on intraplate seismogenesis at high latitudes, *Quat. Sci. Rev.,* **19,** 1399–1411.

Plomerová, J. & Babuška, V., 2010. Long memory of mantle lithosphere fabric—European LAB constrained from seismic anisotropy, *Lithos,* **120,** 131–143.

Popov, Y.A., Pevzner, S.C., Pimenov, V.P. & Romushkevich, R.A., 1999. New geothermal data from the Kola Superdeep well SG-3, *Tectonophysics,* **306,** 345–366.

Puura, V. & Vaher, R., 1997. Deep structure, in *Geology and Mineral Resources of Estonia*, p. 163, eds Raukas, A. & Teedumäe, A., Estonian Academic Publishers.

Ranalli, G., 1995. *Rheology of the Earth,* Springer, p. 414.

Rasilainen, K., Lahtinen, R. & Bornhorst, T.J., 2007. The rock geochemical database of Finland manual, *Geol. Surv. Finland, Rep. Invest.,* **164,** 38.

Rudnick, R.L. & Nyblade, A.A., 1999. The thickness of Archean lithosphere: constraints from xenolith thermobarometry and surface heat flow, in *Mantle Petrology; Field Observations and High Pressure Experimentation: A Tribute to Francis R. (Joe) Boyd*, pp. 3–11, eds Fei, Y., Bertka, C.M. & Mysen, B.O., Geochemical Society.

Rybach, L., 1988. Determination of heat production rate, in *Handbook of Terrestrial Heat Flow Density Determination*, pp. 125–142, eds Haenel, R., Rybach, L. & Stegena, L., Kluwer Academic Publishers.

Rybach, L. & Buntebarth, G., 1984. The variation of heat generation, density and seismic velocity with rock type in the continental lithosphere, *Tectonophysics,* **103,** 335–344.

Schatz, J.F. & Simmons, G., 1972. Thermal conductivity of Earth materials at high temperatures, *J. geophys. Res.,* **77,** 6966–6983.

Scholz, C.H., 1998. Earthquakes and friction laws, *Nature,* **391,** 37–42.

Silvennoinen, H., Kozlovskaya, E., Kissling, E., Kosarev, G. & POLENET/LAPNET Working Group, 2014. A new Moho boundary map for the northern Fennoscandian Shield based on combined controlled-source seismic and receiver function data, *GeoResJ,* **1–2,** 19–32.

Slagstad, T., Balling, N., Elvebakk, H., Midttømme, K., Olesen, O., Olsen, L. & Pascal, C., 2009. Heat-flow measurements in Late Palaeoproterozoic to Permian geological provinces in south and central Norway and a new heat-flow map of Fennoscandia and the Norwegian-Greenland Sea, *Tectonophysics,* **473,** 341–361.

Steffen, H. & Wu, P., 2011. Glacial isostatic adjustment of Fennoscandia – a review of data and modeling, *J. Geodyn.,* **52,** 169–204.

Tanaka, A., 2004. Geothermal gradient and heat flow in and around Japan (II): crustal thermal structure and its relationship to seismogenic layer, *Earth Planets Space,* **56,** 1195–1199.

Tanaka, A. & Ishikawa, Y., 2002. Temperature distribution and focal depth in the crust of northeastern Japan, *Earth Planets Space,* **54,** 1109–1113.

Tanaka, A., Yamano, M., Yano, Y. & Sasada, M., 2004. Geothermal gradient and heat flow in and around Japan (I): appraisal of heat flow from geothermal gradient data, *Earth Planets Space,* **56,** 1191–1194.

Tiira, T., Uski, M., Kortström, J., Kaisko, O. & Korja, A., 2016. Local seismic network for monitoring of a potential nuclear power plant area, *J. Seismol.,* **20,** 397–417.

Torsvik, T.H. & Rehnström, E.F., 2003. The Tornquist Sea and Baltica-Avalonia docking, *Tectonophysics,* **362,** 67–82.

Uski, M., Tiira, T., Grad, M. & Yliniemi, J., 2012. Crustal seismic structure and depth distribution of earthquakes in the Archean Kuusamo region, Fennoscandian Shield, *J. Geodyn.,* **53,** 61–80.

Valtonen, O., Uski, M., Korja, A., Tiira, T. & Kortström, J., 2013. Optimal configuration of a micro-earthquake network, *Adv. Geosci.,* **34,** 33–36.

Vosteen, H.-D. & Schellschmidt, R., 2003. Influence of temperature on thermal conductivity, thermal capacity and thermal diffusivity for different types of rock, *Phys. Chem. Earth,* **28,** 499–509.

Wong, I.G. & Chapman, D.S., 1990. Deep intraplate earthquakes in the western United States and their relationship to lithospheric temperature, *Bull. seism. Soc. Am.,* **80,** 589–599.

Zoth, G. & Haenel, R., 1988. Appendix, in *Handbook of Terrestrial Heat-Flow Density Determination*, pp. 449–466, eds Haenel, R., Stegena, L. & Rybach, L., Springer.

SUPPORTING INFORMATION

Supplementary data are available at *GJI* online.

APPENDICES

The heat flow data used in the study has been gathered in the MS Word file AppendixA.docx and the earthquake data in the MS Excel spreadsheet AppendixB.xlsx, both included in zip package 'appendixes.zip'. Both palaeoclimatically corrected and uncorrected heat flow information has been tabulated. In the seismic data table, the Finnish and Swedish data sets accepted for the analysis, as well as the rejected data from both countries, are provided in the form of spreadsheets with explanations.

Please note: Oxford University Press is not responsible for the content or functionality of any supporting materials supplied by the authors. Any queries (other than missing material) should be directed to the corresponding author for the paper.